Journal of Traditional and Complementary Medicine 14 (2024) 424–434

Contents lists available at ScienceDirect

Journal of Traditional and Complementary Medicine

journal homepage: www.elsevier.com/locate/jtcme

Atractylodes macrocephala Koidz. and *Cuscuta chinensis* Lam. extract relieves insulin resistance via PI3K/Akt signalling in diabetic *Drosophila*

Yinghong Li [a,1], Ye Xu [a,1], Biwei Zhang [a,b], Zhigang Wang [a], Leilei Ma [a,b], Longyu Sun [a], Xiuping Wang [c], Yimin Lin [d], Ji-an Li [a,b,**], Chenxi Wu [a,*]

[a] *Hebei Key Laboratory of Integrated Traditional Chinese and Western Medicine for Diabetes and Its Complications, College of Traditional Chinese Medicine, North China University of Science and Technology, 21 Bohai Road, Tangshan, 063210, China*
[b] *School of Public Health, North China University of Science and Technology, 21 Bohai Road, Tangshan, 063210, China*
[c] *Institute of Coastal Agriculture Hebei Academy of Agriculture and Forestry Sciences, Tangshan, 063299, China*
[d] *First Hospital of Qinhuangdao, 258 Wenhua Road, Qinguangdao, 066000, China*

ARTICLE INFO

Keywords:
Atractylodes macrocephala Koidz
Cuscuta chinensis Lam
Insulin Resistance
Drosophila
PI3K/Akt

ABSTRACT

Background and aim: Type-2 diabetes mellitus (T2DM) is mainly characterized by insulin resistance (IR) induced by hyperglycaemia and insufficient insulin secretion. We employed a diabetic fly model to examine the effect and molecular mechanism of *Atractylodes macrocephala* Koidz. and *Cuscuta chinensis* Lam. (AMK–CCL) extract as traditional Chinese medicine in treating IR and T2DM.

Experimental procedure: The contents of the active ingredients (rhamnose, xylose, mannose, and hyperoside) in AMK–CCL extract were determined by high-performance liquid chromatography. Wild-type (*Cg*-GAL4/+) or diabetic (*Cg* > InR^{K1409A}) *Drosophila* flies were divided into the control group or metformin group and AMK–CCL (0.0125, 0.025, 0.05, 0.1 g/ml) groups. Food intake, haemolymph glucose and trehalose, protein, weight, triglycerides (TAG), and glycogen were measured to assess glycolipid metabolism. Phosphatidylinositol-3-kinase (PI3K)/Akt signalling was detected using fluorescent reporters [tGPH, *Drosophila* forkhead box O (dFoxO)–green fluorescent protein (GFP), *Glut1*–GFP, 2-NBDG] *in vivo*. *Glut1*/3 mRNA levels and Akt phosphorylation levels were detected by quantitative polymerase chain reaction and western blotting, respectively, *in vitro*.

Results: AMK–CCL extract contained 0.038 % rhamnose, 0.017 % xylose, 0.69 % mannose, and 0.039 % hyperoside. AMK–CCL at 0.0125 g/mL significantly suppressed the increase in circulating glucose, and the decrease in body weight, TAG, and glycogen contents of diabetic flies. AMK–CCL improved PI3K activity, Akt phosphorylation, Glut1/3 expression, and glucose uptake in diabetic flies, and also rescued diabetes-induced dFoxO nuclear localisation.

Conclusions: These findings indicate that AMK–CCL extract ameliorates IR-induced diabetes via the PI3K/Akt signalling pathway, providing an experimental basis for clinical treatment.

Abbreviations: AMK, *Atractylodes macrocephala* Koidz.; CCL, *Cuscuta chinensis* Lam.; T2DM, Type-2 Diabetes Mellitus; TCM, traditional Chinese medicine; IR, Insulin Resistance; PI3K, phosphatidylinositol-3-kinase; TAG, Triglycerides; HPLC, high-performance liquid chromatography; dFoxO, *Drosophila* Forkhead Box O; qRT-PCR, quantitative Real-Time PCR; *Rp49*, *Ribosomal protein 49*; 2-NBDG, 2-deoxy-2-[(7-nitro-2,1,3-benzoxadiazol-4-yl) amino]-D-glucose; GLUT, Gucose transporter; DN, dominant-negative; PDK, 3-phosphoinositide-dependent protein kinase; mTORC2, mechanistic target of rapamycin complex 2; GSK3*β*, glycogen synthase kinase 3*β*; TSC2, tuberous sclerosis complex 2; LncRNA, long non-coding RNA.

Peer review under responsibility of The Center for Food and Biomolecules, National Taiwan University.

* Corresponding author.
** Corresponding author. Hebei Key Laboratory of Integrated Traditional Chinese and Western Medicine for Diabetes and Its Complications, College of Traditional Chinese Medicine, North China University of Science and Technology, 21 Bohai Road, Tangshan, 063210, China.
E-mail addresses: JianLi@ncst.edu.cn (J.-a. Li), chenxi.wu@ncst.edu.cn (C. Wu).
[1] These authors contribute equally to this work.

https://doi.org/10.1016/j.jtcme.2024.01.010
Received 19 April 2023; Received in revised form 13 December 2023; Accepted 31 January 2024
Available online 31 January 2024

1. Introduction

Recently, there has been an increase in the number of people with diabetes globally, with type-2 diabetes mellitus (T2DM) accounting for more than 90 % of these cases.[1] T2DM is a chronic metabolic disorder with a high incidence rate, which is mainly characterised by insulin resistance (IR) caused by hyperglycaemia and insufficient insulin secretion.[2] IR is a core defect of T2DM, defined as suppressed sensitivity to the physiological effects of insulin in the body, limiting the ability of insulin to induce its regular biological effects.[3] Therefore, ameliorating IR to prevent and treat diabetes has attracted considerable research attention.

In traditional Chinese medicine (TCM), diabetes is classified into the 'wasting, thirst, and heat' category, characterised by fatigue, polydipsia, polyphagia, and polyuria.[4] Over the years, poor 'spleen' and 'kidney' functions were considered the main causes of wasting and thirsting disease in TCM.[5] Thus, improving spleen and kidney function is a common approach in diabetes prevention and treatment. *Atractylodes macrocephala* Koidz. (AMK; Chinese name, Baizhu) has a bitter-sweet taste and is known to stimulate the spleen and stomach meridian, according to TCM.[6] Modern pharmacological studies have shown that AMK effectively lowers fasting blood sugar and plasma insulin levels and increases the insulin sensitivity index.[7] *Cuscuta chinensis* Lam. (CCL; Chinese name, Tusizi) has a pungent-sweet taste, which is believed to target the liver and kidney meridians in TCM, with the mature seeds being a popular ingredient in medicinal drugs. Previous studies have demonstrated that the CCL polysaccharide and its active ingredient hyperoside can improve the pathological states of polyphagia, polydipsia, polyuria, and weight loss in diabetic rats, as well as lower IR.[8] Therefore, inspired by Xuemin Zhao's *Compendium* (*GangMuShiYi*) in the Qing Dynasty, who used AMK combined with CCK to treat 'weakness and emaciation', we hypothesised that the combination of these two drugs would give full play to their effects of invigorating the spleen and tonifying the kidney, providing a new theoretical basis for the 'simultaneous treatment of the spleen and kidney' in IR and T2DM treatment.

Drosophila melanogaster has become a classic model organism to study different diseases owing to several advantages over other common model organisms (e.g. rats and mice), including low feed cost, rapid speed of reproduction, large number of offspring, short life cycle, simplicity of genetic manipulation, and absence of ethical issues.[9] In particular, *Drosophila* has emerged as an ideal experimental organism for investigating the pharmacodynamics of glucose and lipid metabolism and related diseases.[10,11] The metabolism-related regulation of classic biochemical pathways, signalling pathways, and protein factors are highly conserved between flies and mammals.[12] The insulin-like peptides/insulin receptor (InR)/insulin receptor substrate (IRS) modules and downstream phosphatidylinositol-3-kinase (PI3K)/Akt signalling pathway in *Drosophila* is similar to the insulin/PI3K/Akt signalling pathway in humans based on functions and modes of regulation.[13–15] In contrast to the common high-calorie diet-induced diabetic model, the *Cg* > InR^{K1409A} diabetic fly model is established by ectopically expressing a dominant-negative form of InR (*UAS*-InR^{K1409A}) specifically in the fat body (equivalent to the mammalian adipose tissue and liver) by a GAL4/UAS expression system.[16] This misdirected expression of InR^{K1409A} interferes with the physiological functions of endogenous InR, thereby reducing the activity of insulin signalling and causing IR. Accordingly, this model was considered to be suitable to explore the influence of drugs or active ingredients on IR more specifically. In addition, recent *in-silico* techniques have been applied to improve the exploration of the molecular mechanisms of diseases and provide new directions for treatment.[17–20]

Therefore, to test our hypothesis, we employed the well-established *Cg* > InR^{K1409A} *Drosophila* diabetic model to explore the effect and underlying molecular mechanism of AMK–CCL extract against IR and T2DM, providing an experimental foundation for a potential TCM-based therapeutic strategy in the clinical treatment of diabetes and associated diseases.

2. Material and methods

2.1. AMK–CCL extract preparation

The two TCM herbs, AMK and CCL (Fig. 1A and B), were purchased from Beijing Tongrentang Tangshan Chain Store Drug Store Co., Ltd. and identified by Professor Li Ji-an at North China University of Science and Technology. The manufacturer and batch number of each crude herb are listed in Supplementary Table 1. AMK and CCL extracts[21,22] were prepared in accordance with ancient records using modern Chinese medicine extraction methods. Briefly, 100 g of AMK and 100 g of CCL were weighed, separately ground into a coarse powder, and soaked in 1 L of 40 % ethanol for 48 h, followed by filtration of the infusion solution and centrifugation at 4200×*g* for 2 h at 25 °C. The supernatant was extracted for subsequent use, and the remaining residues were decocted with 1 L of deionised water for 1 h, followed by filtration and centrifugation at 4200×*g* for 4 h. The two supernatants from both processes were mixed at a ratio of 1:1 and filtered using a 0.45-μm sieve. The extract (0.4 g/mL) was retrieved for subsequent use (Fig. 1C; Supplementary Fig. 1).

2.2. Quality control by high-performance liquid chromatography (HPLC)

The quality of the AMK–CCL extract was assessed according to the contents of the primary active ingredients rhamnose, xylose, mannose, and hyperoside. Standard compounds were obtained from the National Institutes for Food and Drugs Control. The contents of each compound were determined on a Shimadzu LC-20A HPLC system equipped with an Agilent Eclipse XDB-C18 column (4.6 mm × 250 mm, 5 μm). The mobile phase flow rate was 1 mL/min and the column temperature was 40 ± 1 °C. The mobile phase for rhamnose, xylose, and mannose detection was acetonitrile (A) and 0.02 mol/L ammonium acetate solution (B) (A: B = 20:80), and the measurement wavelength was 250 nm. The mobile phase of hyperoside detection was acetonitrile (C) and 0.1 % phosphoric acid solution (D) (C:D = 17:83), and the measurement wavelength was 360 nm.[6]

2.3. Drosophila strains and treatments

Flies were maintained on a standard sucrose/cornmeal-based medium (1000 mL basal medium preparation: 50 g sucrose, 60 g corn flour, 10 g agar, 30 g yeast, 6 mL propionic acid, and 1000 mL double-distilled water) at 25 °C in a 12-h light-dark cycle incubator with 55–65 % relative humidity. The *Drosophila* stocks w^{1118} (#3605), *Cg*-GAL4 (#7011), *UAS*-InR^{K1409A} (#8253), tGPH (#8164), *dFoxO*-GFP (#37585), $Glut1^{MI02222}$ (#33178), and $Glut1^{MB01560}$ (#23196) were obtained from Bloomington *Drosophila* Stock Centre. The crossing scheme for all groups is shown in Supplementary Fig. 2.

To determine the anti-diabetic effect of the AMK–CCL extract, flies with the *Cg* > InR^{K1409A} genotype (diabetic model) were raised from the fertilized ovum/egg stage to third-instar larval stage in medium containing AMK–CCL or metformin (Met) as a positive control. The prepared AMK–CCL extract was directly mixed into the basal food at a concentration of 0.0125, 0.025, 0.05, or 0.1 g/mL. Flies in control and model groups were maintained on the standard basal-medium diet, while those in the Met (10 mM)[16,23] and AMK–CCL (0.0125, 0.025, 0.05, or 0.1 g/mL) groups were maintained in media containing the treatments at the respective levels approximately 6 days before all samples were collected and analysed. All crossing assays were performed using healthy, unmated male and female parents.

2.4. Food intake

Since the addition of the drugs could potentially influence energy intake and directly affect the metabolism of the organism, we examined

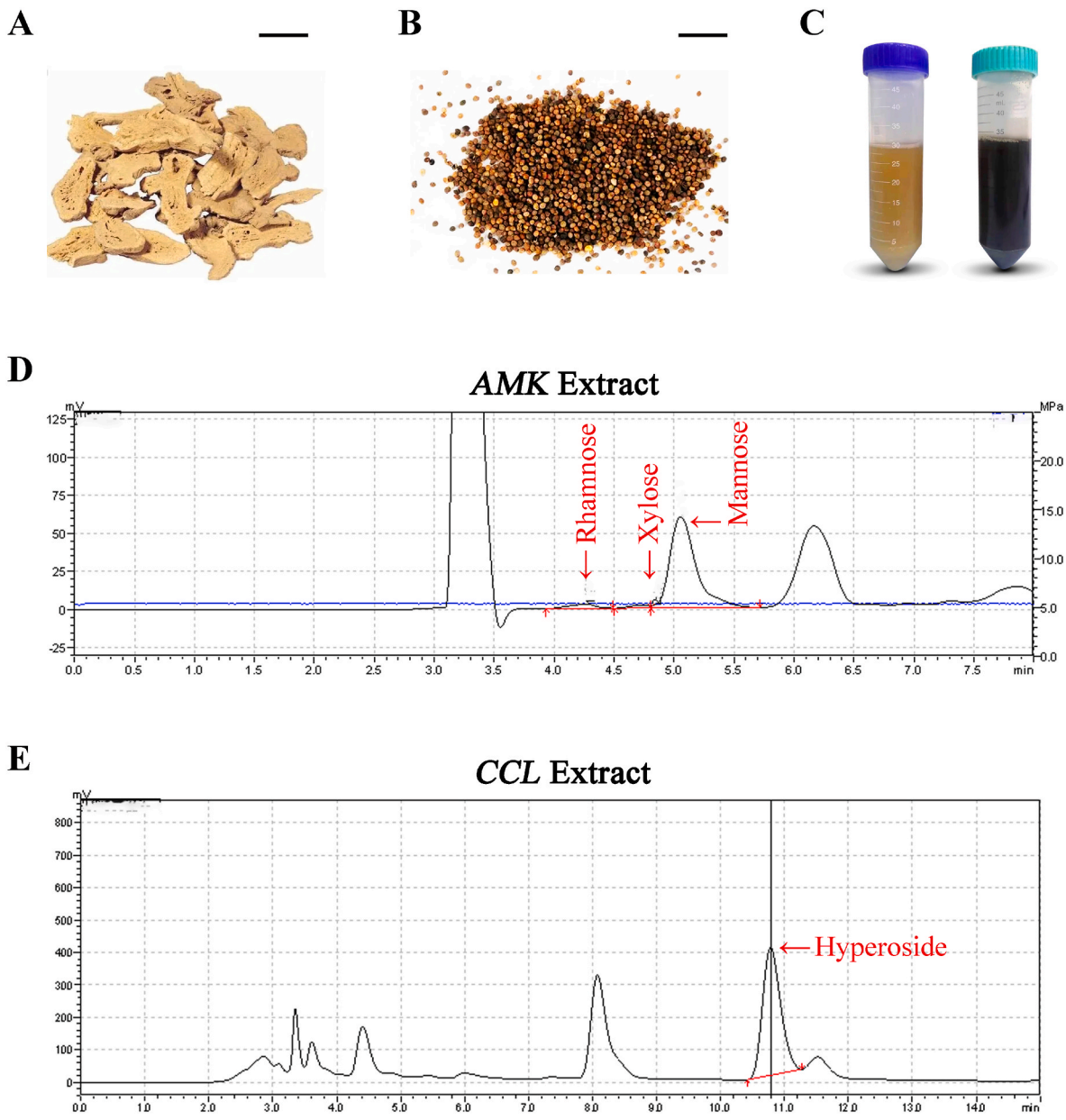

Fig. 1. High-performance liquid chromatography (HPLC) analysis of AMK-CCL. Photographs of *Atractylodes macrocephala Koidz* (AMK, Baizhu), (**A**) *Cuscuta chinensis Lam* (CCL, Tusizi) (**B**), and their extracts in centrifuge tubes (**C**). HPLC chromatograms of the AMK extract (**D**) and CCL extract (**E**). Four major compounds were identified and compared with the standards using HPLC. Rhamnose, xylose, mannose, and hyperoside were identified using HPLC. The detection wavelengths for rhamnose, xylose, mannose (**D**, 250 nm) and hyperoside (**E**, 360 nm) with peaks indicated by red arrows.

the potential influence of the drugs on food intake using the wild-type strain w^{1118}. Early third-instar larvae were starved for 2 h under adverse food conditions (0.8 % agar in phosphate-buffered saline [PBS]) and then transferred to a medium containing 0.5 % Brilliant Blue FCF (Blue-9) dye for 20 min. Thereafter, the larvae were washed with PBS and homogenised in an EP tube containing 100 μL lysis buffer using a micro high-speed homogeniser. After centrifuging for 3 min using a high-speed refrigerated centrifuge, 2 μL of the obtained supernatant was used to determine feed intake at 630 nm.[24]

2.5. Haemolymph glucose and trehalose measurement

Third-instar larvae were collected, rinsed with PBS, dried on tissue paper, and the cuticle was carefully torn to release the haemolymph. Haemolymph (2 μL) was collected using a micropipette, diluted 20 times with cold PBS, and centrifuged for 3 min at a rotation speed of 12,700. The supernatant was boiled at 75 °C for 10 min and removed by centrifugation. Glucose was measured after 15 min of incubation at 37 °C using HK reagent (Sigma, #G3293) and detected on a plate reader at 340 nm. Trehalose was converted using porcine trehalase (Sigma, #T8778) overnight at 37 °C, and the total amount of glucose was measured following the steps described above.[16]

2.6. Protein, triglycerides (TAG), and glycogen measurements

Third-instar larvae were collected and rinsed several times with PBS to remove traces of food. The samples were homogenised using a pellet pestle in 200 μL of cold 0.05 % PBST (PBS + 0.05 % Tween-20) on ice, followed by heat inactivation at 75 °C for 10 min and subsequent cooling to 25 °C. Thereafter, the samples were homogenised in an EP tube containing 100 μL of lysis buffer using a high-speed homogeniser. The protein content of the homogenate (10 μL) was determined using a

bicinchoninic acid assay protein assay kit (Beyotime, #P0010).

For TAG content determination, 10 μL of the homogenate was mixed with 10 μL of triglyceride reagent (Sigma, #T2449) containing lipase for TAG-to-glycerol hydrolysis at 37 °C for 60 min, followed by centrifugation for 3 min at a rotation speed of 12,700. Subsequently, 10 μL of the supernatant was used for the measurement of TAG using free glycerol reagent (Sigma, #F6428) at 540 nm. The TAG concentration was determined by subtracting the values of free glycerol from the untreated samples.

To determine the glycogen content, 5 μL of the homogenate was incubated with 10 μL of buffer A [5 mM of Tris-HCl (pH 6.6), 137 mM of NaCl, and 2.7 mM of KCl] containing amyloglucosidase (Sigma, #10115) at 50 °C for 60 min to digest glycogen. Ten microliters of the homogenate were incubated with 5 μL of buffer A without enzymes in parallel for the determination of glucose levels. The glycogen concentration was determined by subtracting the values of free glucose from the untreated samples. The amounts of TAG and glycogen were normalised to the soluble protein content.[16,25]

2.7. Immunostaining

The larval fat body tissues were dissected and fixed in 4 % formaldehyde for 20 min at 25 °C. After several washes with 0.3 % PBST, the samples were stained with primary antibody at 4 °C overnight, followed by incubation with secondary antibodies at 25 °C for 2 h. The following antibodies were used: mouse anti-Dlg1 (1:100, Developmental Studies Hybridoma Bi, #4F3 anti-discs large) and goat anti-mouse-Cyanine3 (Cy3) (1:1000, Life Technologies, #A10521). Vectashield medium (Vector Laboratories, #H-1500) with 4′,6-diamidino-2-phenylindole (DAPI) was used for mounting.

2.8. Western blotting

Whole larvae were lysed in radioimmunoprecipitation assay buffer (Beyotime, #P0013) containing phosphatase inhibitor cocktail A (Beyotime, #P1082) and phenylmethanesulfonyl fluoride. Equal amounts of protein were separated by sodium dodecyl sulphate-polyacrylamide gel electrophoresis, transferred to a polyvinylidene fluoride membrane, and subjected to the standard western blot protocol as previously described.[26] The following antibodies were used for incubation: anti-Akt (1:1000, Cell Signalling Technology (CST), #4691], rabbit anti-p-Akt (Ser505) (1:2000, CST, #4060), rabbit p-Akt (Thr342) (1:500, Invitrogen, PA5-95669), rabbit anti-α-tubulin (1:1000, CST, #2125), and goat anti-rabbit IgG (H + L, HRP) (1:10000, Sera Care, #5220-0336).

2.9. Reverse transcription-quantitative polymerase chain reaction (RT-qPCR)

TRIzol (Invitrogen) and RNAeasy™ Animal RNA Isolation Kit (Beyotime R0026) were used to isolate total RNA from eight third-instar larvae of different groups, and RT-qPCR was performed as previously described.[27] Ribosomal protein 49 (*Rp49*) was used as the reference gene. The primer sequences are shown in Supplementary Table 3.

2.10. Glucose uptake assay

Third-instar larvae were dissected in PBS, followed by incubation with 2-deoxy-2-[(7-nitro-2,1,3-benzoxadiazol-4-yl) amino]-D-glucose (2-NBDG, $C_{12}H_{14}N_4O_8$) (Invitrogen N13195) at 0.3 mM for 15 min in the dark at 29 °C.[28] After rinsing with PBS, rapid dissection of fat body tissues, and covering with a coverslip, images were acquired with a fluorescence microscope (Olympus, IX51).

2.11. Data analysis

All data were verified using at least three independent experiments. Results are presented as bar graphs constructed using GraphPad Prism 8.0 software. One-way analysis of variance with Bonferroni's multiple-comparison test was used to determine statistical significance between groups. Mean values were considered statistically significant with differences at $p < 0.05$. The error bars indicate standard deviations.

3. Results

3.1. Metabolic profile of AMK–CCL extract

A comparison of AMK–CCL HPLC chromatograms with those of the standards (Supplementary Fig. 3) indicated distinct peaks for rhamnose, xylose, mannose, and hyperoside in the chemical fingerprints of the AMK–CCL extract (Fig. 1D and E). The rhamnose, xylose, mannose, and hyperoside contents of the AMK–CCL extract were 0.038 %, 0.017 %, 0.69 %, and 0.039 %, respectively (Table 1; Supplementary Table 2), indicating that the extract contained essential active ingredients and was suitable for use in further *in vivo* experiments.

3.2. AMK–CCL extract ameliorates glycolipid metabolism disorder in diabetic flies (*Cg* > InR^{K1409A})

A *Drosophila* IR diabetic model was generated by expressing a dominant-negative (DN) form of *Drosophila* InR (*UAS*-InR^{K1409A}) under the control of the fat body-specific collagen (*Cg*) promoter GAL4 to elucidate the effect of AMK-CCL extract on T2DM and IR.[16] Consistent with our previous findings, expression of the InR antimorphic allele (*UAS*-InR^{K1409A}) under the control of *Cg*-Gal4 (*Cg* > InR^{K1409A}) interfered with the physiological function of endogenous InR and undermined the downstream response of the insulin signalling cascade, resulting in a significant increase in haemolymph glucose and trehalose levels in diabetic flies (*Cg* > InR^{K1409A}) (Fig. 2B and C). We found no significant difference in ingestion rates between the control, Met, and AMK–CCL groups (Fig. 2A), thereby ruling out the possibility that the metabolic phenotypes may be due to changes in feeding rate. The *Cg* > InR^{K1409A}-induced increase in circulating glucose levels was significantly suppressed by Met and 0.0125 g/mL of AMK–CCL extract (Fig. 2B). In contrast, no concentration of AMK–CCL extract suppressed the *Cg* > InR^{K1409A}-induced increase in circulating trehalose in *Drosophila* at the larval stage (Fig. 2C).

Compared with those of the control group, pupal body weight and the larval protein content were significantly lower in the diabetes model group (Fig. 2D; Supplementary Fig. 4). However, treatment with Met or 0.0125, 0.025, and 0.1 g/mL of AMK–CCL significantly rescued diabetes-induced weight loss (Fig. 2D); moreover, treatment with 0.1 g/mL of the AMK–CCL extract reversed the diabetes-induced decrease in protein content (Supplementary Fig. 4). Compared with those of the control group, TAG and glycogen contents were significantly lower in the diabetes model group (Fig. 2E and F). However, treatment with Met or 0.0125 and 0.025 g/mL of the AMK–CCL extract significantly rescued the diabetes-induced decrease in TAG content (Fig. 2E). Moreover, treatment with only 0.0125 and 0.025 g/mL of the AMK–CCL extract

Table 1
HPLC analysis of *AMK–CCL* representative active components.

Sample name	Retention time (min)	Area	Height	Concentration (mg/mL)	Proportion (%)
Rhamnose	4.255	38358	2725	0.364	0.038
Xylose	4.804	21255	1847	0.170	0.017
Mannose	5.055	905660	59919	7.148	0.69
Hyperoside	10.784	7798911	392863	0.394	0.039

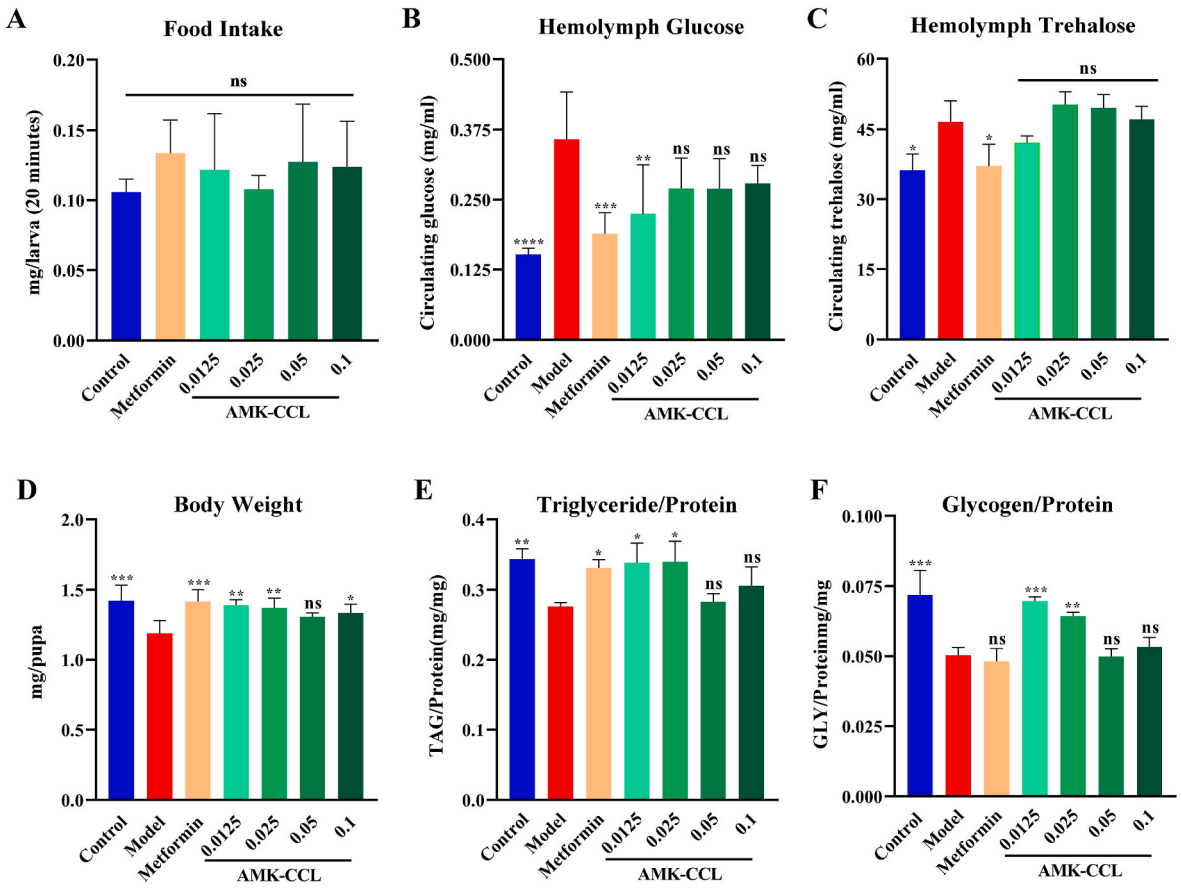

Fig. 2. AMK-CCL ameliorates glycolipid metabolism disorder in diabetic *Cg* > InR^{K1409A} flies. (**A**) Determination of food intake by early third-instar larvae was calculated using blue-stained food (containing Blue-9) (6–8 larvae per pool, n = 5). (**B**, **C**) Assays for circulating metabolites were performed on third-instar larvae: haemolymph glucose (10–12 larvae per pool, n = 5) (**B**), and haemolymph trehalose (6–8 larvae per pool, n = 3) (**C**). (**D**) Pupal body weight (n = 5). Determination of triglyceride (TAG) (**E**) and glycogen contents (**F**) at the third-instar larval stage (three larvae per pool, n = 3). TAG and glycogen contents were presented relative to the protein contents of the tissue sample to normalise the weight difference between the control and other indicated groups (three larvae per pool, n = 3). Error bars indicate standard deviation (S.D.). Statistical difference was calculated using one-way ANOVA and Bonferroni's multiple comparison test: ****$p < 0.0001$, ***$p < 0.001$, **$p < 0.01$, and *$p < 0.05$; ns: no significant difference.

significantly improved the diabetes-induced decrease in glycogen content (Fig. 2F). Based on these results, 0.0125 g/mL of AMK–CCL extract was selected for further experiments.

3.3. AMK-CCL improves PI3K activity in vivo

The effect of the AMK–CCL extract on PI3K activation and insulin signalling was examined using an *in situ* fluorescent reporter termed tGPH (a fusion protein containing a tubulin promoter, GFP, and a PH domain), which recognises 3,4,5-phosphatidyl-triphosphate (PIP_3) and helps to visualise PI3K activation.[29] Compared with those of the control group, the fat body cells (equivalent to mammalian adipose and liver tissues) of the IR model displayed decreased GFP cell membrane localisation, indicating a decrease in PI3K activity (Fig. 3A-A‴, B–B‴). However, an increase in the GFP signal was observed in the membrane after treatment with AMK–CCL extract or Met, indicating enhanced PI3K activity (Fig. 3C-C‴, D-D‴). Overall, these results indicated that treatment with the AMK–CCL extract improved PI3K transduction activity to ameliorate IR.

3.4. AMK–CCL promotes Akt phosphorylation

To elucidate the effect of AMK–CCL on PI3K/Akt signalling, we monitored Akt phosphorylation using western blotting analysis. Consistent with previous findings,[16] ectopic expression of the InR^{K1409A} allele in the larval fat body of *Cg* > InR^{K1409A} flies caused a decrease in Akt phosphorylation (p-Akt) levels at both the Thr342 and Ser505 sites (equivalent to Thr308 and Ser473 in mammalian Akt1[26,30]) compared with those of the control group (Fig. 4A–D). Treatment with AMK–CCL or Met significantly suppressed the diabetes-induced decreases in p-Akt expression levels (Fig. 4A–D), whereas the total expression level of Akt was unaffected by the treatment. Overall, these data suggested that AMK–CCL increased Akt phosphorylation.

3.5. AMK–CCL extract inhibits Drosophila FoxO (dFoxO) transfer from the cytoplasm to the nucleus

Since dFoxO is a key downstream transcription factor of the PI3K/Akt pathway, the effect of AMK–CCL on the subcellular localisation of the *dFoxO*-GFP fusion protein in fat body cells was examined.[31] When InR^{K1409A} was expressed in fat body cells under the control of *Cg*-GAL4, the nuclear localisation of *dFoxO-GFP* was largely increased (Fig. 5A-A‴, B–B‴). However, treatment with AMK–CCL extract or Met inhibited the nuclear localisation of *dFoxO*-GFP (Fig. 5C- C‴, D-D‴). Overall, these data indicated that the AMK–CCL extract promoted the cytoplasmic localisation of dFoxO.

3.6. AMK–CCL extract elevates Glut1 expression

Glucose transporter (GLUT) proteins, encoded by solute carriers 2A genes, are the primary factors responsible for sugar uptake in all mammalian cells.[32,33] Among them, GLUT1 is the main transporter

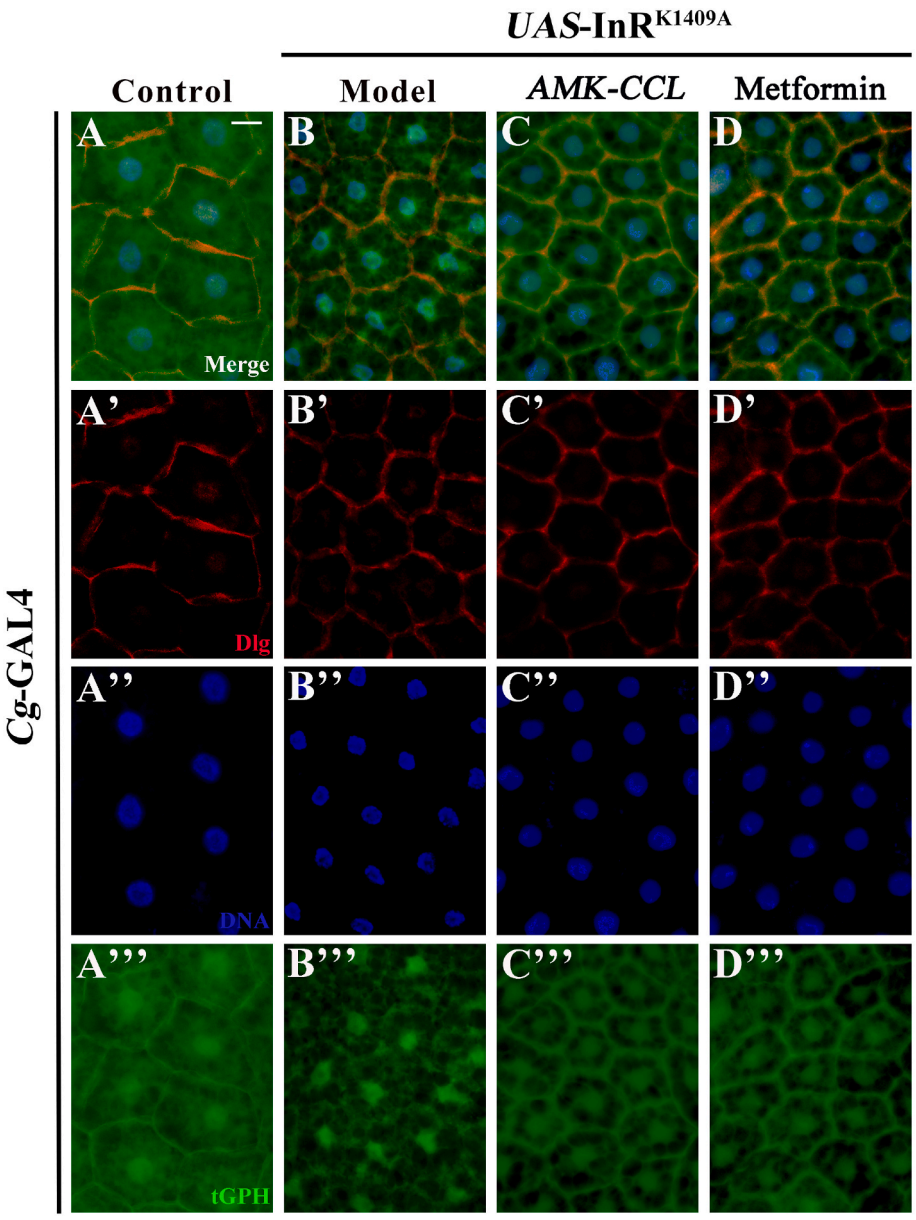

Fig. 3. AMK-CCL extract promotes PI3K activity *in vivo*. (**A**–**D**) Merged fluorescence micrographs showing the third-instar larval fat body carrying tGPH reporter stained with anti-Dlg, outlining the cell membrane. The individual channels detected only Dlg (red, A′-D′), only DNA (blue, A″-D″, labelled with DAPI), and only tGPH signals (green, A‴-D‴, PI3K activity). Scale bar: 25 μm. Genotypes: (**A**) *Cg*-GAL4/+; tGPH/+, (**B**–**D**) *Cg*-GAL4/+; tGPH/*UAS*-InR^{K1409A}.

responsible for glucose uptake. In *Drosophila*, Glut1 is the closest homolog of human GLUT1 with 68 % sequence similarity, which is ubiquitously expressed in target tissues with strong expression in neurons.[34–36] As the expression of Glut1 is mainly regulated by the upstream PTEN/Akt signal,[37,38] we introduced the *Glut1*^{MI02222} strain that carries a MiMIC insertion in the intron preceding the last coding exon and takes along the green fluorescent protein (GFP) marker (*Glut1*-GFP) to monitor the *in situ* expression of *Drosophila* Glut1 and explore the effect of AMK–CCL on glucose uptake.[39,40] We further employed the *Glut1*^{MB01560} strain with the MiET1 insertion accompanied by a GFP marker.[41] In the control group, the Glut1 protein was found extensively in the plasma membrane of fat body cells, as visualized by the *Glut1*^{MI02222} (Fig. 6A-A″) or *Glut1*^{MB01560} strain (Supplementary Fig. 5A-A″). The expression level of Glut1 was strongly reduced in the *Cg* > InR^{K1409A}-induced diabetic model (Fig. 6B-B″; Supplementary Fig. 5B-B″), which was then markedly elevated following treatment with AMK–CCL extract or Met (Fig. 6C-C″, D-D″; Supplementary Fig. 5C-C″, D-D″). Moreover, RT-qPCR showed that compared with those of the control, the reduced mRNA levels of *Glut1* and *Glut3* in *Cg* > InR^{K1409A} larvae were remarkably improved by treatment with AMK–CCL extract or Met (Fig. 6E and F). Collectively, these results indicated that AMK–CCL extract reverses IR-induced down-regulated expression of Glut factors.

3.7. AMK–CCL extract drives glucose uptake in the Drosophila fat body

As glucose uptake is the well-recognized functional role of GLUT1, we monitored glucose uptake in third-instar larval fat body cells *in vivo* using the fluorescence-labelled glucose analogue 2-NBDG (Fig. 7F).[42] As expected, we observed massive green fluorescent dots in the normal control group (Fig. 7A-A″), indicating that 2-NBDG was internalized through glucose transporters, similar to glucose. Although the transportation of 2-NBDG into cells was distinctively impeded in the diabetic model larvae (Fig. 7B-B″), increased import of 2-NBDG was found in the

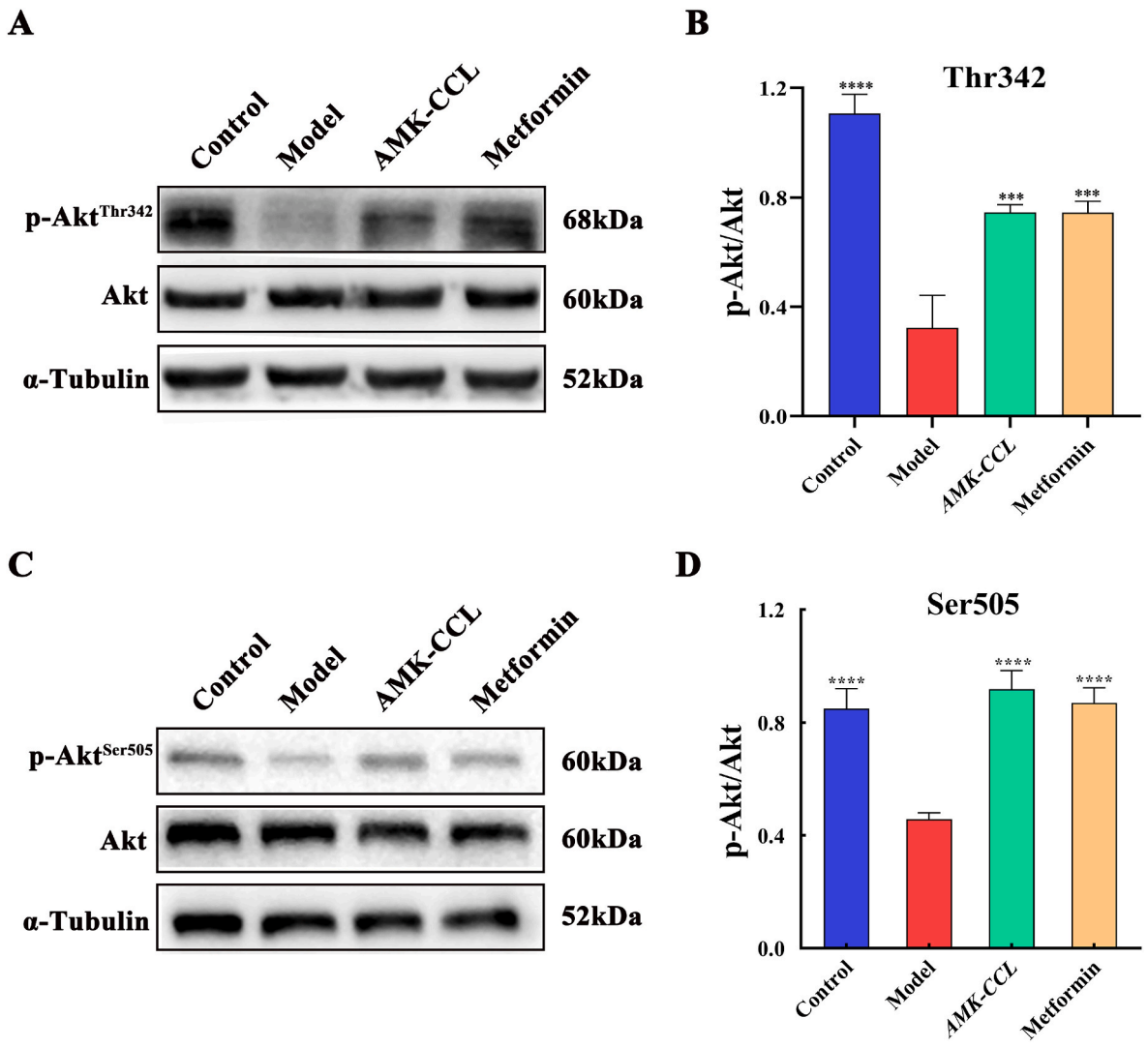

Fig. 4. AMK-CCL increases Akt phosphorylation level. (**A** and **C**) Western blot analysis of whole-body extracts from third-instar larvae for phosphorylated Akt (p-Akt) and total Akt, with α-tubulin as the loading control (nine larvae per time). Groups (from left to right): control (*Cg*-GAL4/+), model (*Cg* > InR^{K1409A}), AMK-CCL (*Cg* > InR^{K1409A} files treated with 0.0125 g/mL of AMK-CCL), and metformin (*Cg* > InR^{K1409A} files treated with metformin) groups. (**B** and **D**) Bar chart of p-Akt/Akt relative levels from three independent experiments shown in **A** and **C**. Error bars indicate standard deviation. Statistical significance was determined using one-way ANOVA with Bonferroni's multiple comparison test; ****$p < 0.0001$; ***$p < 0.001$.

AMK–CC extract and Met groups (Fig. 7C-C″, D-D″ and E). Taken together, these data confirmed that AMK–CCL extract could help drive glucose uptake to ameliorate IR-induced diabetes.

4. Discussion

IR is the pathological cause of T2DM, which predominantly manifests as abnormal insulin signalling in the target tissues of insulin, such as the muscle, liver, and fat. The InR/PI3K/Akt/FoxO signalling pathway is the major pathway of insulin signalling.[13–15] For the past two decades, *Drosophila melanogaster* has been widely used to study different diseases and processes, including IR-induced diabetes and drug molecular mechanisms,[43,44] owing to advantages of the highly conserved regulatory system for maintaining the circulating sugar balance from flies to humans,[45,46] the powerful genetic manipulation tools available, and the reduced genome redundancy.[47,48] Therefore, we used the *Cg* > InR^{K1409A} diabetic fly model to explore the influence of AMK–CCL extract on IR to provide an experimental foundation for the broad application of this TCM in diabetes treatment and management.

Notably, the multi-component and multi-target synergistic effect of TCM can significantly improve the prognosis of patients with diabetes, and inhibit the progress of IR through anti-inflammatory, anti-oxidation, and anti-bacterial mechanisms.[49–51] AMK has been shown to improve glucose metabolism, and its main molecular mechanism involves the regulation of IR and mitogen-activated protein kinase signalling pathways. The main active ingredients of AMK are volatile oil, polysaccharides, and sesquiterpene lactone compounds.[52] Wang et al.[53] further identified rhamnose, mannose, xylose, and galactose as important constituents of polysaccharides in AMK. Among them, D-xylose (regarded as a sucrase inhibitor) regulates blood glucose levels in the body via regeneration of damaged tissue of the pancreas and liver and regulates the key rate-limiting enzyme in gluconeogenesis, PEPCK.[54] Moreover, crude polysaccharide and rhamnose-enriched polysaccharides have been reported to increase body weight and pancreatic insulin levels and to decrease blood glucose levels of diabetic rats, indicating that rhamnose-enriched polysaccharide acts as a potent anti-diabetic agent, suggesting its potential in the development of an alternative medicine for diabetes.[55] As a key effective component of CCL, hyperoside has been reported to inhibit high glucose-induced oxidative stress injury in myocardial cells through activation of the PI3K/Akt/Nrf2 signalling pathway.[56] Vermaet al.[57] demonstrated that hyperoside plays a key role in regulating blood sugar levels by

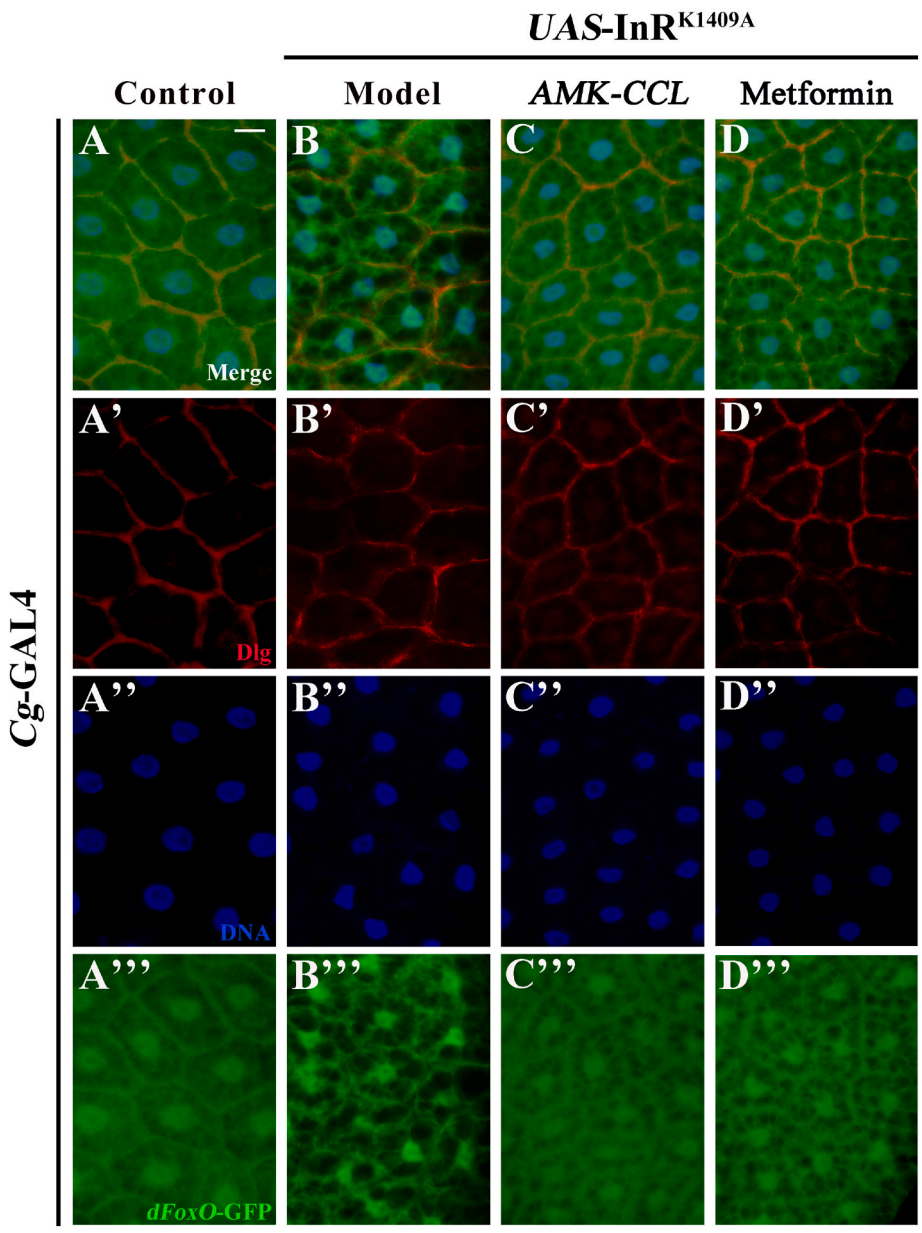

Fig. 5. AMK-CCL rescues *Cg* > InR^{K1409A}-induced dFoxO nuclear localisation. (**A**–**D**) Representative merged fluorescence micrographs showing the third-instar larval fat body carrying *dFoxO*-GFP reporter. The individual channels detected only Dlg (red, A′-D′), only DNA (blue, A″-D″), and only *dFoxO*-GFP (green, A‴-D‴). Scale bar: 25 μm. Genotypes: (**A**) *Cg*-GAL4/+; *dFoxO*-GFP/+, (**B**–**D**) *Cg*-GAL4/+; *dFoxO*-GFP/*UAS*-InR^{K1409A}.

improving islet function, increasing glycolysis, and reducing gluconeogenesis. Moreover, network pharmacology analysis showed that the main active constituents of CCL, including β-sitosterol, kaempferol, matrine, isopropanol, and quercetin, can regulate key target proteins (EGFR, MMP9, and VEGFA) and are concentrated in five signalling pathways, including the PI3K/Akt pathway. Among these pathways, multiple active components act on Akt1 and ESR1 to improve glucose metabolism.[58]

Consistent with these previous findings, our HPLC analysis of the AMK–CCL extract showed that the contents of rhamnose, xylose, mannose, and hyperoside were 0.038 %, 0.017 %, 0.69 %, and 0.039 %, respectively. These four effective components might play a role through PI3K/Akt signalling either alone or synergistically in improving IR, increasing PI3K activity, and regulating the intracellular localisation of FoxO *in vivo*. Among the four concentrations tested, 0.0125 g/mL AMK–CCL extract displayed the most effective inhibition effect on IR in the *Cg* > InR^{K1409A} diabetes model. Based on the quantification of *Drosophila* daily food intake and the drug dose conversion between *Drosophila* and humans,[59–61] it is estimated that flies raised on a medium containing 0.0125 g/mL of AMK–CCL is comparable to a treatment dosage of 26 g (AMK 13 g, CCL 13 g) per day for human patients. In the clinic, the recommended dosage of both AMK and CCL is 6–12 g in *China Pharmacopoeia*, 2020 Edition. Thus, taking 0.0125 g/mL AMK-CCL for a fly (equivalent to 26 g/day for a human) is approximately in the upper line of the normal dosage range (24 g/day), which complies with the principle of drug safety and suitability.

We examined the anti-diabetic effect of AMK–CCL extract with an emphasis on insulin signalling, demonstrating that the extract could increase body weight, protein, glycogen, and triglyceride contents, while decreasing circulating glucose levels in the *Drosophila Cg* > InR^{K1409A} diabetic model. In addition to these basic biochemical effects, the AMK–CCL extract enhanced PI3K transduction activity, Akt phosphorylation (at both Thr342 and Ser505, corresponding to Thr308 and Ser473 in mammalian Akt1[26,30]), Glut1 expression in the plasma

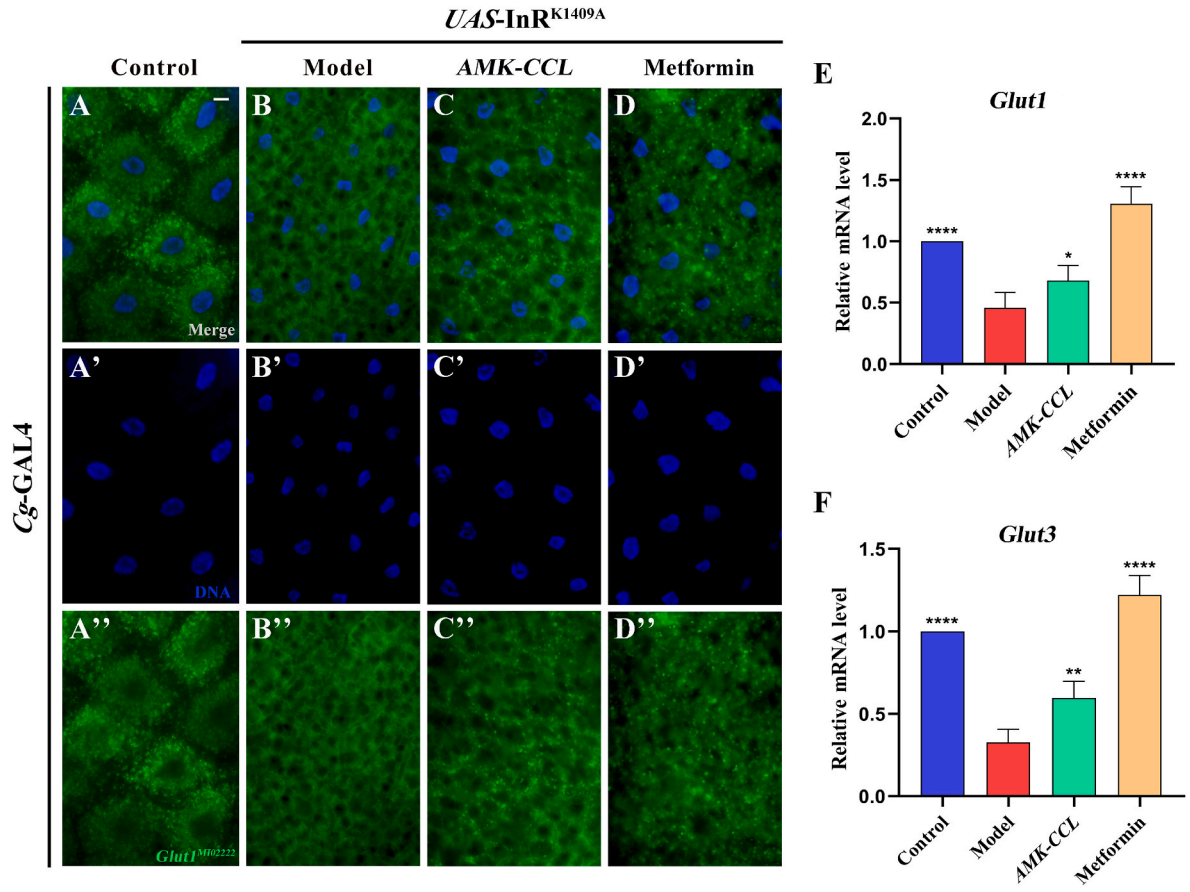

Fig. 6. AMK–CCL extract improves the expression of glucose transporters. (**A**–**D**) Representative merged fluorescence micrographs of the third-instar larval fat body carrying the *Glut1*^{MI02222} (*Glut1*-GFP) reporter. The individual channels detected only DNA (blue, A′-D′) and only *Glut1*^{MI02222} (*Glut1*-GFP) (green, A″-D″). Scale bar: 20 μm. Genotypes: (**A**) *Cg*-GAL4/+; *Glut1*^{MI02222}/+, (**B**–**D**) *Cg*-GAL4/+; *Glut1*^{MI02222}/*UAS*-InR^{K1409A}. mRNA levels of *Glut1* (**E**) and *Glut3* (**F**), as measured by RT-qPCR (n = 4). Error bars represent the standard deviation. One-way analysis of variance with Bonferroni's multiple comparison test was used to compute *p*-values: ****$p <$ 0.0001, **$p < 0.01$, and *$p < 0.05$.

membrane, and glucose uptake, while inhibiting the nuclear localisation of dFoxO. Except for the p-Akt level, which was determined by the western blot assay *in vitro*, the other metabolic indices were all confirmed using GFP-labelled reporters *in vivo*, including tGPH (for PI3K activity), *dFoxO*-GFP, *Glut1*-GFP, and 2-NBDG (for glucose uptake). In insulin signal transduction, activated InR could phosphorylate IRS after binding by insulin on the target cell surface, which in turn phosphorylates PI3K to catalyse the generation of PIP_3 inositol from 4,5-bisphosphate phosphatidylinositol (PIP_2). PIP_3 then recruits both 3-phosphoinositide-dependent protein kinase (PDK) and Akt to the cell membrane, where PDK and mechanistic target of rapamycin complex 2 (mTORC2) phosphorylate Akt at T308 and S473, respectively. The fully activated Akt with double phosphorylation subsequently phosphorylates and regulates the downstream transcription factors (such as FoxO, glycogen synthase kinase 3*β*, and tuberous sclerosis complex 2), thereby mediating glucose and lipid metabolism.[46,62,63] Among these steps, Glut protein-mediated glucose uptake constitutes a key physiological reaction.[34] Thus, the activities of these central factors (i.e. PI3K, Akt, FoxO, Glut) are closely related to abnormal glycolipid metabolism, providing key clues for the application of AMK–CCL in the clinical management of diabetes and other related diseases.

There are some limitations of this study. Firstly, AMK and CCL contain numerous active ingredients with anti-diabetic effects, and we only tested the contents of rhamnose, xylose, mannose, and hyperoside by HPLC. Therefore, further exploration is needed to determine the specific ingredients that play a major role in the observed anti-diabetes effects. Secondly, considering the adverse reactions or side effects of drugs, follow-up studies should focus on the potential long-term effects of drug intervention. Thirdly, diabetes is a complex disease with other multiple contributing factors and pathways, including the role of *β*-cells, autophagy, long non-coding RNAs, glucagon signalling, WNT signalling, and others.[63–65] It is therefore important to determine whether the molecular mechanism of AMK–CCL in improving diabetes is conserved between flies and humans and to consider potential broader therapeutic approaches accordingly. Despite the above limitations, this work nevertheless provides preliminary data for further study on the clinical application of AMK–CCL in treating IR and T2DM.

5. Conclusions

The combination of AMK and CCL (0.0125 g/mL) was found to reduce circulating glucose levels and increase stored energy in a *Drosophila* diabetic model. Furthermore, this treatment positively regulated PI3K/Akt/FoxO signalling, improving IR. These findings provide a theoretical basis for the potential use of the extract from AMK and CCL in the treatment of diabetes.

Financial support

This work was supported by Science and Technology Partnership Program, Ministry of Science and Technology of China (KY201904005), and Hebei Natural Science Foundation (H2023209038) to Ji-an Li, Hebei Natural Science Foundation (H2022209027), Tangshan Science and Technology Project (21130230C) and Tangshan Talent Funding

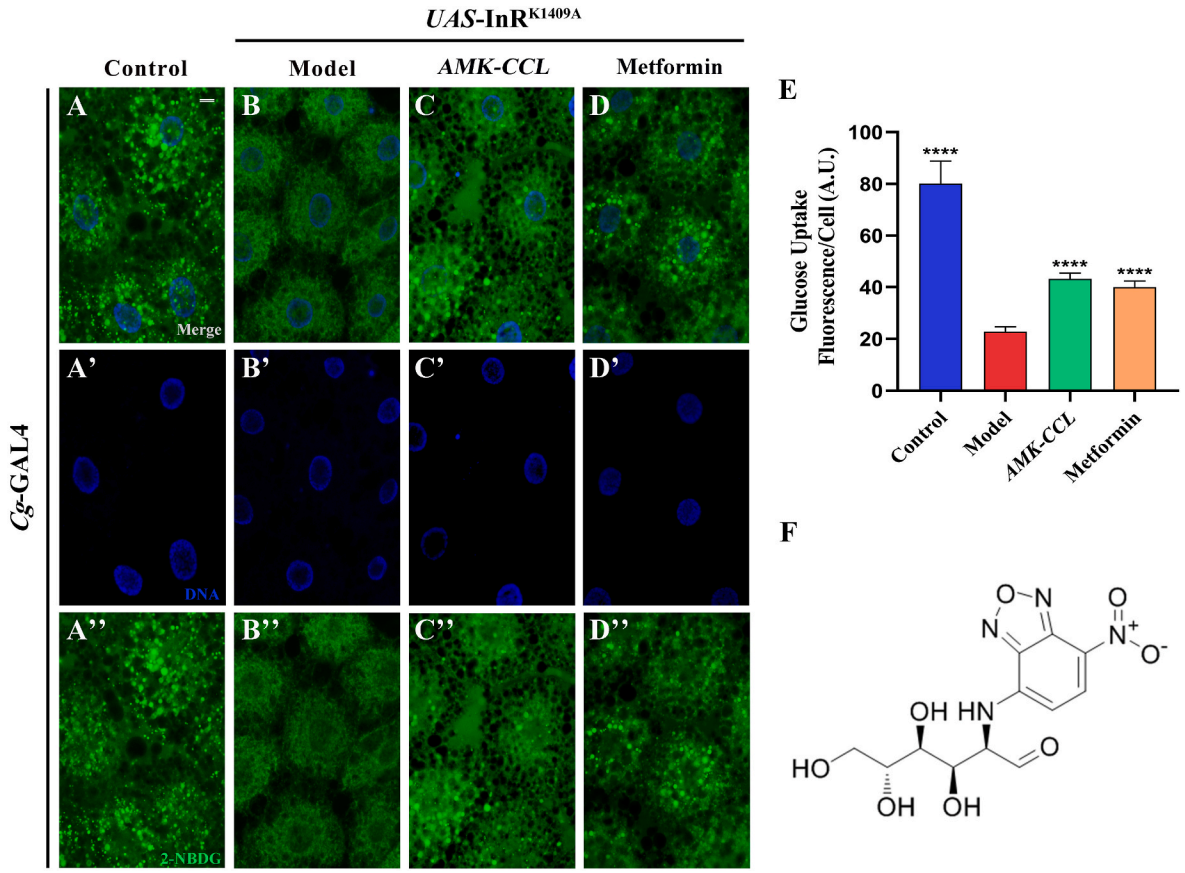

Fig. 7. AMK–CCL relieves glucose intake. (**A**–**D**) Glucose incorporation (marked by 2-NBDG uptake) levels in the third-instar larval fat body. The individual channels detected only DNA (blue, A′-D′) and only 2-NBDG (green, A″-D″). Scale bar: 20 μm. Genotypes: (**A**) *Cg*-GAL4/+, (**B**–**D**) *Cg*-GAL4/+; *UAS*-InR^{K1409A}/+. (**E**) ImageJ quantitation of the glucose uptake (fluorescence intensity per cell, n = 10). Error bars represent the standard deviation. One-way analysis of variance with Bonferroni's multiple comparison test was used to compute *p*-values: ****$p < 0.0001$; ns: no significant difference ($p > 0.05$). (**F**) Chemical structure of 2-NBDG.

Project (A202203021) to Chenxi Wu, Hebei Provincial Administration of Traditional Chinese Medicine Scientific Research Project (2020222) to Biwei Zhang, Basic Research Funds of Hebei Academy of Agriculture and Forestry Sciences (2022KJCXZX-BHS-4) to Xiuping Wang.

Data availability

The original contributions presented in the study are included in the article/Supplementary Material. Further inquiries can be directed to the corresponding authors.

Declaration of competing interest

The authors declare no conflict of interest.

We declare that we do not have any commercial or associative interest that represents a conflict of interest in connection with the work submitted.

Acknowledgements

We thank Bloomington *Drosophila* Stock Center for the fly stocks, and members of the Wu and Li lab for discussion and critical comments.

Appendix A. Supplementary data

Supplementary data to this article can be found online at https://doi.org/10.1016/j.jtcme.2024.01.010.

References

1. International Diabetes Federation. *IDF Diabetes Atlas*. tenth ed. Brussels: International Diabetes Federation; 2021.
2. Lee SH, Park SY, Choi CS. Insulin resistance: from mechanisms to therapeutic strategies. *Diabetes Metab J*. 2022;46:15–37.
3. Pomytkin I, Pinelis V. Brain insulin resistance: focus on insulin receptor-mitochondria interactions. *Life*. 2021;11:262.
4. Liu X, Wu QQ, Shi Y, et al. Theoretical framework of diabetic names based on traditional Chinese medicine literature. *Chin Arch Trad Chin Med*. 2020;38:199–202.
5. Ding L, Zhu XY, Peng JY, et al. Effect of Jianpi Yishen recipe on nutritional status and immune function of diabetic patients. *Chin Arch Trad Chin Med*. 2022;40:72–74.
6. National Pharmacopoeia Commission. *Chinese Pharmacopoeia*. Beijing: China Medical Science and Technology Press; 2020.
7. Chao CL, Huang HC, Lin HC, et al. Sesquiterpenes from Baizhu stimulate glucose uptake by activating AMPK and PI3K. *Am J Chin Med*. 2016;44:963–979.
8. Zhang Y, Wang M, Dong H, et al. Anti-hypoglycemic and hepatocyte-protective effects of hyperoside from *Zanthoxylum bungeanum* leaves in mice with high-carbohydrate/high-fat diet and alloxan-induced diabetes. *Int J Mol Med*. 2018;41:77–86.
9. Yamaguchi M, Yoshida H. Drosophila as a model organism. *Adv Exp Med Biol*. 2018;1076:1–10.
10. Rulifson EJ, Kim SK, Nusse R. Ablation of insulin-producing neurons in flies: growth and diabetic phenotypes. *Science*. 2002;296:1118–1120.
11. Tennessen JM, Barry WE, Cox J, et al. Methods for studying metabolism in Drosophila. *Methods*. 2014;68:105–115.
12. Ugur B, Chen K, Bellen HJ. Drosophila tools and assays for the study of human diseases. *Dis Model Mech*. 2016;9:235–244.
13. Biglou SG, Bendena WG, Chin-Sang I. An overview of the insulin signaling pathway in model organisms *Drosophila melanogaster* and *Caenorhabditis elegans*. *Peptides*. 2021;145, 170640.
14. Huang X, Liu G, Guo J, et al. The PI3K/AKT pathway in obesity and type 2 diabetes. *Int J Biol Sci*. 2018;14:1483–1496.
15. Lee S, Dong HH. FoxO integration of insulin signaling with glucose and lipid metabolism. *Internet J Endocrinol*. 2017;233:R67–R79.

16. Cao X, La X, Zhang B, et al. Sanghuang tongxie formula ameliorates insulin resistance in Drosophila through regulating PI3K/Akt signaling. *Front Pharmacol*. 2022;13, 874180.
17. Kumar A, Rajendran V, Sethumadhavan R, Purohit R. In silico prediction of a disease-associated STIL mutant and its affect on the recruitment of centromere protein J (CENPJ). *FEBS Open Bio*. 2012;2:285–293.
18. Kumar Bhardwaj V, Purohit R, Kumar S. Himalayan bioactive molecules as potential entry inhibitors for the human immunodeficiency virus. *Food Chem*. 2021;347, 128932.
19. Rajendran V. Structural analysis of oncogenic mutation of isocitrate dehydrogenase 1. *Mol Biosyst*. 2016;12(7):2276–2287.
20. Rajendran V, Sethumadhavan R. Drug resistance mechanism of PncA in Mycobacterium tuberculosis. *J Biomol Struct Dyn*. 2014;32(2):209–221.
21. Hu Y, Li XZ, Liu Y, et al. Study on quality standard of cuscuta extract. *Liquor-making Sci Technol*. 2021:42–47.
22. Yang Y, Wei MX, Wu YY, et al. Research progress on extraction separation, chemical constitution and pharmacological activities of polysaccharide extracted from Atractylodes macrocephala. *Chin Tradit Herb Drugs*. 2021;52:578–584.
23. Shirazi F, Farmakiotis D, Yan Y, et al. Diet modification and metformin have a beneficial effect in a fly model of obesity and mucormycosis. *PLoS One*. 2014;9, e108635.
24. Hiroko M, Takayuki Y, Miki Y, et al. Flies without trehalose. *J Biol Chem*. 2015;290, 1255-1255.
25. Li H, Tennessen JM. Methods for studying the metabolic basis of *Drosophila* development. *Wiley Interdiscip Rev Dev Biol*. 2017;6, e290.
26. Roth SW, Bitterman MD, Birnbaum MJ, et al. Innate immune signaling in Drosophila blocks insulin signaling by uncoupling PI(3,4,5)P(3) production and Akt activation. *Cell Rep*. 2018;22:2550–2556.
27. Wang MC, Bohmann D, Jasper H. JNK signaling confers tolerance to oxidative stress and extends lifespan in *Drosophila*. *Dev Cell*. 2003;5:811–816.
28. Wong KKL, Liao JZ, Verheyen EM. A positive feedback loop between Myc and aerobic glycolysis sustains tumor growth in a *Drosophila* tumor model. *Elife*. 2019;8, e46315.
29. Britton JS, Lockwood WK, Li L, Cohen SM, Edgar BA. *Drosophila*'s insulin/PI3-kinase pathway coordinates cellular metabolism with nutritional conditions. *Dev Cell*. 2002;2:239–249.
30. Sharma S, Mathre S, Ramya V, Shinde D, Raghu P. Phosphatidylinositol 5 phosphate 4-kinase regulates plasma-membrane PIP(3) turnover and insulin signaling. *Cell Rep*. 2019;27:1979–1990.
31. Wu C, Chen Y, Wang F, et al. Pelle modulates dFoxO-mediated cell death in *Drosophila*. *PLoS Genet*. 2015;11, e1005589.
32. Holman GD. Structure, function and regulation of mammalian glucose transporters of the SLC2 family. *Pflügers Archiv*. 2020;472:1155–1175.
33. Ismail A, Tanasova M. Importance of GLUT transporters in disease diagnosis and treatment. *Int J Mol Sci*. 2022;23:8698.
34. de Tredern E, Rabah Y, Pasquer L, Minatchy J, Plaçais PY, Preat T. Glial glucose fuels the neuronal pentose phosphate pathway for long-term memory. *Cell Rep*. 2021;36, 109620.
35. Escher SA, Rasmuson-Lestander A. The *Drosophila* glucose transporter gene: cDNA sequence, phylogenetic comparisons, analysis of functional sites and secondary structures. *Hereditas*. 1999;130:95–103.
36. Vittori A, Breda C, Repici M, et al. Copy-number variation of the neuronal glucose transporter gene SLC2A3 and age of onset in Huntington's disease. *Hum Mol Genet*. 2014;23:3129–3137.
37. Morani F, Phadngam S, Follo C, et al. PTEN regulates plasma membrane expression of glucose transporter 1 and glucose uptake in thyroid cancer cells. *J Mol Endocrinol*. 2014;53:247–258.
38. Phadngam S, Castiglioni A, Ferraresi A, Morani F, Follo C, Isidoro C. PTEN dephosphorylates AKT to prevent the expression of GLUT1 on plasmamembrane and to limit glucose consumption in cancer cells. *Oncotarget*. 2016;7:84999–85020.
39. Volkenhoff A, Hirrlinger J, Kappel JM, Klämbt C, Schirmeier S. Live imaging using a FRET glucose sensor reveals glucose delivery to all cell types in the *Drosophila* brain. *J Insect Physiol*. 2018;106:55–64.
40. Nagarkar-Jaiswal S, Lee PT, Campbell ME, et al. A library of MiMICs allows tagging of genes and reversible, spatial and temporal knockdown of proteins in *Drosophila*. *Elife*. 2015;4, e05338.
41. Bellen HJ, Levis RW, He Y, et al. The *Drosophila* gene disruption project: progress using transposons with distinctive site specificities. *Genetics*. 2011;188:731–743.
42. O'Neil RG, Wu L, Mullani N. Uptake of a fluorescent deoxyglucose analog (2-NBDG) in tumor cells. *Mol Imag Biol*. 2005;7:388–3892.
43. Graham P, Pick L. *Drosophila* as a model for diabetes and diseases of insulin resistance. *Curr Top Dev Biol*. 2017;121:397–419.
44. Wang L, Kounatidis I, Ligoxygakis P. *Drosophila* as a model to study the role of blood cells in inflammation, innate immunity and cancer. *Front Cell Infect Microbiol*. 2014;3:113.
45. Baker KD, Thummel CS. Diabetic larvae and obese flies-emerging studies of metabolism in *Drosophila*. *Cell Metabol*. 2007;6:257–266.
46. Alfa RW, Kim SK. Using *Drosophila* to discover mechanisms underlying type 2 diabetes. *Dis Model Mech*. 2016;9:365–376.
47. Cox JE, Thummel CS, Tennessen JM. Metabolomic studies in *Drosophila*. *Genetics*. 2017;206:1169–1185.
48. Germani F, Bergantinos C, Johnston LA. Mosaic analysis in *Drosophila*. *Genetics*. 2018;208:473–490.
49. Pang GM, Li FX, Yan Y, et al. Herbal medicine in the treatment of patients with type 2 diabetes mellitus. *Chinese Med J*. 2019;132:78–85.
50. Cui X, Qian DW, Jiang S, Shang EX, Zhu ZH, Duan JA. Scutellariae Radix and Coptidis Rhizoma improve glucose and lipid metabolism in T2DM rats via regulation of the metabolic profiling and MAPK/PI3K/Akt signaling pathway. *Int J Mol Sci*. 2018;19:3634.
51. Zhu Y, Li Y, Liu M, Hu X, Zhu H. Guizhi Fuling Wan, Chinese herbal medicine, ameliorates insulin sensitivity in PCOS model rats with insulin resistance via remodeling intestinal homeostasis. *Front Endocrinol*. 2020;11:575.
52. Liu C, Wang S, Xiang Z, et al. The chemistry and efficacy benefits of polysaccharides from *Atractylodes macrocephala* Koidz. *Front Pharmacol*. 2022;13, 952061.
53. Wang R, Zhou G, Wang M, Peng Y, Li X. The metabolism of polysaccharide from *Atractylodes macrocephala* Koidz and its effect on intestinal microflora. *Evid Based Complement Alternat Med*. 2014;2014, 926381.
54. Kim E, Kim YS, Kim KM, Jung S, Yoo SH, Kim Y. D-Xylose as a sugar complement regulates blood glucose levels by suppressing phosphoenolpyruvate carboxylase (PEPCK) in streptozotocin-nicotinamide-induced diabetic rats and by enhancing glucose uptake in vitro. *Nutr Res Prac*. 2016;10:11–18.
55. Seedevi P, Ramu Ganesan A, Moovendhan M, et al. Anti-diabetic activity of crude polysaccharide and rhamnose-enriched polysaccharide from *G. lithophila* on streptozotocin (STZ)-induced in Wistar rats. *Sci Rep*. 2020;10:556.
56. Wang C, Li X, Liu Z, Han ML, Hou YL, Guo CL. The effect and mechanism of hyperoside on high glucose-induced oxidative stress injury of myocardial cells. *Sichuan Da Xue Xue Bao Yi Xue Ban*. 2018;49:518–523.
57. Verma N, Amresh G, Sahu PK, Mishra N, Rao CV, Singh AP. Pharmacological evaluation of hyperin for antihyperglycemic activity and effect on lipid profile in diabetic rats. *Indian J Exp Biol*. 2013;51:65–72.
58. Yu Y, Zhang G, Han T, et al. Effect of cuscutae semen on the type-2 diabetes mellitus based on network pharmacology and molecule docking method. *Chinese J Clin Pharmacol*. 2020;36:813–817.
59. Deshpande SA, Carvalho GB, Amador A, et al. Quantifying *Drosophila* food intake: comparative analysis of current methodology. *Nat Methods*. 2014;11:535–540.
60. Slack C, Alic N, Foley A, Cabecinha M, Hoddinott MP, Partridge L. The Ras-Erk-ETS-signaling pathway is a drug target for longevity. *Cell*. 2015;162:72–83.
61. Wang S, Wu F, Ye B, et al. Effects of Xuefu Zhuyu Decoction on cell migration and ocular tumor invasion in *Drosophila*. *BioMed Res Int*. 2020, 5463652, 2020.
62. Goberdhan DC, Wilson C. The functions of insulin signaling: size isn't everything, even in *Drosophila*. *Differentiation*. 2003;71:375–397.
63. Demir S, Nawroth PP, Herzig S, Ekim Üstünel B. Emerging targets in type 2 diabetes and diabetic complications. *Adv Sci*. 2021;8, e2100275.
64. Jin T. The WNT signalling pathway and diabetes mellitus. *Diabetologia*. 2008;51:1771–1780.
65. Guo H, Wu H, Li Z. The pathogenesis of diabetes. *Int J Mol Sci*. 2023;24:6978.